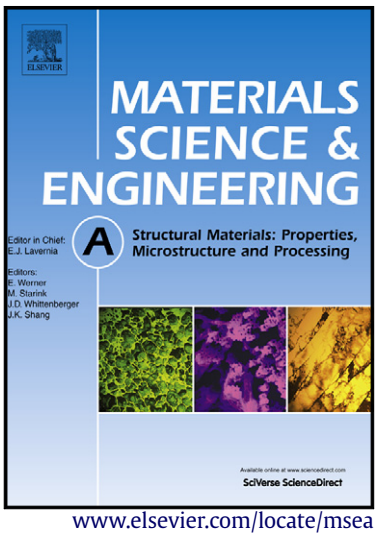

www.elsevier.com/locate/msea

A Multiscale Approach for the Deformation Mechanism in Pearlite Microstructure Numerical Evaluation of the Elasto-plastic Deformation in Fine Lamellar Structures

Tetsuya Ohashi, Lidyana Roslan, Kohsuke Takahashi, Tomotsugu Shimokawa, Masaki Tanaka, Kenji Higashida

PII: S0921-5093(13)01008-3
DOI: http://dx.doi.org/10.1016/j.msea.2013.09.032
Reference: MSA30285

To appear in: *Materials Science & Engineering A*

Cite this article as: Tetsuya Ohashi, Lidyana Roslan, Kohsuke Takahashi, Tomotsugu Shimokawa, Masaki Tanaka, Kenji Higashida, A Multiscale Approach for the Deformation Mechanism in Pearlite Microstructure Numerical Evaluation of the Elasto-plastic Deformation in Fine Lamellar Structures, *Materials Science & Engineering A,* http://dx.doi.org/10.1016/j.msea.2013.09.032

A Multiscale Approach for the Deformation Mechanism in Pearlite Microstructure

Numerical Evaluation of the Elasto-plastic Deformation in Fine Lamellar Structures

Tetsuya Ohashi [1*], Lidyana Roslan [1], Kohsuke Takahashi [1], Tomotsugu Shimokawa [2], Masaki Tanaka [3], and Kenji Higashida [3]

[1] Kitami Institute of Technology, Kitami Japan,
[2] Kanazawa University, Kanazawa Japan,
[3] Kyusyu University, Fukuoka Japan

*e-mail: ohashi@newton.mech.kitami-it.ac.jp,
Phone: +81-(0)157-26-9227,
Postal address: Kitami Institute of Technology, Koencho 165, Kitami, Hokkaido, 0908507, Japan

Abstract

Elasto-plastic deformations in the microstructures of pearlite are studied by finite element analyses. A variety of models for the lamellar structure are made and material properties of cementite and ferrite are established. Deformation of a bare specimen of cementite is unstable immediately after the yield point, while cementite lamellae show some stability when they are layered with ferrite. When higher values of yield stress and strain hardening are used for ferrite phase, cementite deforms well beyond the elastic range and distribution of plastic strain is not concentrated. These results show that not only the layered structure but also improved mechanical property of fine lamellae of ferrite contribute largely to stable deformation in pearlite microstructure.

Keywords
finite element method; steel; plasticity; shear bands; pearlite

1. Introduction

Elasto-plastic deformation in the microstructure of pearlite phase in steels has been a point of interest especially due to the fact that strength and ductility coexist in the pearlitic steels. In the microstructure, fine layers of ferrite and cementite are piled up repeatedly at intervals of sub-micrometer. Under an external load, stress states in the ferrite and cementite were found to differ largely [1]; however the detailed aspects of plastic deformation in each phase remains unknown.

Mechanical properties of single phase specimens of ferrite or cementite with the size at an order of millimeters were investigated experimentally[2,3]. When the experiment was performed at room temperature, the plastic flow stress of pure-ferrite specimens was at the order of a few hundred MPa and the elongation was larger than 20%, while the elastic limit of specimens of single phase cementite was revealed to be approximately 3 GPa and brittle fracture took place immediately after the elastic limit.

Deformation of cementite layers in the microstructure of pearlite has also been studied extensively[4–7] and it was shown that cementite lamellar do deform plastically in pearlite microstructure. Therefore, one most crucial question is why the cementite can deform plastically in the microstructure [8]. Understandings of the mechanics and mechanism of plastic deformation in the pearlite microstructure will lead to the understandings of the reason for the coexistence of strength and ductility in the steels with pearlite phase.

Stability of elasto-plastic deformation of laminated structure was studied by Inoue *et al*. [9] and they showed that fracture stress and elongation increased with decrease of layer thickness, and recently, Serror and Inoue [10] studied the effect of hardening exponent and other parameters of the ductile component to the stability of laminated structure. In this paper, we study the elasto-plastic deformation in the lamellar structure of pearlite from a viewpoint of computational solid mechanics. A variety of finite element-models for the lamellar structure are made and material properties of each phase are established based on existing experimental data and on theoretical possibilities. Unidirectional tensile loading in the direction parallel to the ferrite-cementite interface is considered. This condition mimics the mechanical state in high strength steel wires used in engineering applications. Stable deformation of cementite layers is discussed from the viewpoints of multi-layering effect with ferrite layers and a possible change of mechanical properties of ferrite phase which should arise from the fact that plastic deformation is confined in a sub-micrometer sized space between cementite layers.

2. Numerical models for multi-layered structure of pearlite

We employ a classical theory of the elasto-plastic deformation of metals where the onset of plastic deformation is defined by the yield condition of von Mises,

$$\sigma_{eq.} - \sigma_Y = 0 . \qquad (1)$$

σ_Y and $\sigma_{eq.}$ denote the yield stress of the material and the equivalent stress, respectively. The ferrite phase hardens after the yield point in an isotropic manner, while the cementite phase is assumed to deform plastically without hardening; i.e. the plastic flow stress of cementite is a constant during plastic deformation. We use a commercial software package of ANSYS [11] for the finite element analysis where the elasto-plastic deformation is analyzed by incremental procedure and under an assumption of associated flow rule. The fact that the cementite phase does not harden during plastic deformation means that its plastic deformation can be highly unstable [12]. To follow this situation by the numerical analysis, we made a number of trial analyses and finally introduced a large number of loading steps where a typical increment of nominal strain during one analysis step is at the order of 10^{-9}. If we introduce larger strain increment, numerical analysis often ends in failure.

Fig. 1 shows a schematic illustration of a five-layered pearlite model. The central layer is always cementite (denoted as Fe_3C) in this study and layers of ferrite (denoted as α) and other cementite are stacked in *y*-direction. Volume fractions of the cementite and ferrite layers are close to 0.5; however the value differs from model to model depending on the number of layers. The mid part of the central layer of cementite is slightly thinned[1] [13] to mimic possible geometrical non-uniformity in real structure of pearlite [14,15].

Young's modulus and yield stress of cementite are 181 GPa and 2.75 GPa, respectively [3]. Poisson's ratio of cementite is assumed to be 0.3. When this material is deformed by uniaxial tensile load, the elastic strain at the yield point is about 1.519%. Experimental results of stress-strain relationship of ferrite was given by Umemoto [2] in the following equation of Swift type [16],

$$\sigma = a(b + \varepsilon^{(p)})^n \qquad (2)$$

[1] Shape of the interfaces between the central layer of Fe_3C and α is given by a cosine function $\delta\cos(2\pi x / L)$, where δ and L are 0.5% of the layer thickness and lateral length of the layer, respectively. The thinnest part of the cementite layer is positioned at x=0 and the thickness is 98% of the original one.

where σ and $\varepsilon^{(p)}$ denote stress and plastic strain, respectively, while *a*, *b* and *n* are constants. Young's modulus and Poisson's ratio of ferrite are assumed to be 200 GPa and 0.3, respectively.

Strengthening mechanism of ferrite lamellae has been discussed from the view points of simple rule of mixture for fiber structure, dispersion strengthening, boundary strengthening, solid solution hardening and dislocation forest hardening [17,18]. Among various mechanisms involved, the boundary strengthening contributes largely. It is well known as the Hall-Petch relationship that mechanical response of metal polycrystals changes as a function of the mean diameter of crystal grains. This means that mechanical response of materials depends on the representative length scale of the microstructure. This scale effect is especially significant when the length scale is smaller than 1 μm. Typical thickness of ferrite layer in pearlite is smaller than 100 nm and its plastic flow stress is anticipated to have a strong scale effect, as similar to the case in ultrafine-grained polycrystals [19] or micrometer sized specimen [20]. Experimental results [21] showed that yield stress of pearlite increased with decrease of the layer thickness of ferrite, and recent theoretical and numerical approach [22,23] showed that the critical resolved shear stress for slip deformation as well as the strain hardening ratio increased rapidly when the plastic slip deformation was confined in volumes of smaller length scale. We introduce such kind of scale effect of mechanical response of ferrite layer *a priori* and introduce hypothetical curves of stress-strain relationship by using the Swift equation with a modification,

$$\sigma = a(b + \varepsilon^{(p)})^n + c, \tag{3}$$

where a constant *c* is introduced artificially to give a higher flow stress level in small length-scale specimen.

Table 1 shows material parameters and numerical constants for the modified Swift equation (3) used in this study. Data for the material named ferrite-org are taken from experimental results by Umemoto [2] while data for materials named ferrite5, ferrite10 and ferrite5n are defined by multiples of the parameters *a* and *n* for the ones for ferrite-org. Flow stress of the material named ferrite5n500 is 500 MPa higher than that of ferrite5n, while the strain hardening ratios for ferrite5n and ferrite5n500 are the same.
Stress-strain curves of cementite and five ferrite materials are shown in Fig. 2. Yield stress and strain hardening rate of the ferrite5 and ferrite10 are high compared to the one for the ferrite-org. Yield stresses of the ferrite5n and ferrite5n500 are higher than that of ferrite-org, while their strain hardening rate is lower.

These hypothetical stress strain relations of ferrite layers in the pearlite lamellar structure is considered to be partially supported by experimental facts [18] that the dislocation density in ferrite layers monotonically increases from the initial value of

7.5×10^{13} m^{-2} to a value larger than 1×10^{16} m^{-2} after deformation up to tensile strain of 3.6. This implies that ferrite layers sandwiched by cementite layers have a significant ability of strain hardening. Effects of this ability are examined by introductions of ferrite5 or ferrite10. There is still another possibility that the flow stress level of ferrite is high due to a narrow space between cementite layers while strain hardening is kept low for some reason. We study the mechanical response of such structures by introducing ferrite5n or ferrite5n500.

Numerical specimens of single layer (cementite only), and 3 through 9-layer models are constructed. Only the mid layer of cementite is slightly thinned as described above. In the following sections of 3.1 and 3.2, condition of symmetricity is introduced and only 1/4 of the specimen, that is the part $x \geq 0, y \geq 0$, is analyzed to reduce the size of numerical data, while in the section 3.3, the entire specimen is analyzed to understand the deformation as a whole. It will be shown in the section 3.3 that the deformation is approximately symmetric with respect to the *x* and *y* axes with some slight non-symmetric behaviors after the onset of shear banding. These non-symmetric behaviors are considered to originate from the unstable nature of the deformation.

Analyses are performed with two-dimensional plane stress assumption with large deformation framework. Specimens are divided into square or nearly square finite elements whose typical size is about 1/8 of the layer thickness. Quadrilateral 8-node elements are used. A uniform tensile displacement is given to the nodes on the lateral surfaces at $x = +/- L/2$. Approximately uniaxial tensile deformation takes place at the initial stage of deformation, and then plastic deformation grows in the specimen.

3. Results and discussion

3.1 Deformation of bare cementite specimen and three-layered specimen of ferrite-org/cementite/ferrite-org

Figs. 3(a)-(c) show distributions of the normal plastic strain component in the loading direction observed in the single layered specimen when the nominal tensile strain are 1.500, 1.504 and 1.508%, respectively. Plastic deformation does not take place in the specimen when the nominal strain is 1.500% and shortly after this stage, some shear bands are formed at the central part of the specimen. This result shows that the plastic deformation in single-layered cementite is nearly unstable and the development of shear bands is extremely rapid.

Fig. 4(a)-(d) show close-up views of the development of plastic shear bands at the central part of the three-layered ferrite-org/cementite/ferrite-org model. Plastic deformation in the cementite layer starts when the nominal tensile strain is 1.5068% and develops toward the ferrite layer. It is noted however, that the value of the plastic strain in the shear bands when the nominal tensile strain is 1.51% (Fig. 4(c)) is smaller than

0.5% and this is much smaller than that obtained in the single-layered cementite (Fig. 3(c)). That is, ferrite layers effectively suppress the unstable deformation of cementite. Fig. 5(a) and (b) compare distributions of normal plastic strain component in the tensile direction observed in the bare cementite and the three-layered models when the nominal tensile strain is 1.7%. Plastic strain in the shear band regions in the model of bare cementite (Fig. 5(a)) is larger than that in the shear bands in three-layered model (Fig. 5(b)) and the localized shear deformation in the three-layered specimen is transferred into the ferrite region. Suppression of localized shear deformation by stacking of ferrite and other cementite layers is discussed in the section 3.3.

3.2 Deformation of specimens with layers of cementite and hypothetical ferrite

Fig. 6(a)-(e) show distributions of normal plastic strain component in the tensile direction in five different specimens where cementite layer is sandwiched by ferrite-org, ferrite5n, ferrite5n500, ferrite5, or ferrite10. These specimens are three layered and the nominal tensile strain is 1.55%. Let us compare Figs. 6(a), (b) and (c) and refer to Fig. 2. In the specimen with ferrite5n or with ferrite5n500, shear bands are formed in the cementite layer even though the yield stresses of these ferrite layers are much higher than that of ferrite-org. This suggests that ferrite layers with higher yield stress but lower strain hardening characteristics do not contribute to the suppression of shear banding of cementite layer; instead, distribution of plastic strain in the ferrite layer is localized more than that in the model with ferrite-org layer.

Aspects of plastic deformation in the cementite layer drastically change when the strain-hardening ratio and the yield stress of the ferrite layer increase as shown in Figs. 6(d) and (e). Plastic strain distributes more or less uniformly in the cementite layer. The maximum value of the plastic strain in the cementite layer is smaller than 0.2% and this is about 1/20 of the value observed in Fig. 6(a), (b) and (c). This means that plastic deformation of cementite layer is effectively stabilized if the strain hardening ratio and yield stress of ferrite layers are sufficiently large.

Fig. 7 shows numerical results of nominal stress vs. nominal strain relations obtained for the bare cementite and five types of three-layered specimens. Bare cementite specimen shows a sudden drop of nominal stress just after the yield point. Before the sudden drop, the gradient of the stress-strain relation is approximately equal to the value of Young's modulus of 181 GPa. This again shows that the bare cementite specimen deformed in a purely elastic manner at first and then instable plastic deformation took place in a very short period of time.

Gradient of the stress-strain relationship of the three-layered ferrite-org/cementite/ferrite-org specimen is close to 95 GPa at first. This value is much smaller than the Young's modulus for cementite or ferrite-org, showing that plastic deformation took place at a very early stage of deformation. When the nominal strain is

at about 1.51 %, the gradient of the stress-strain relationship turns out to be negative; however, the stress-strain curve shows some stability compared to the bare cementite specimen.

Deformation curve of the three-layered specimens with ferrite10 shows three stages of deformation. First, the gradient of the deformation curve is slightly larger than 181 GPa, showing that both ferrite and cementite layers are in elastic state. Plastic deformation starts in ferrite layers when the nominal strain is at about 0.5%. After this onset of plastic deformation in ferrite layers, the gradient of the deformation curve becomes smaller. This deformation state lasts until the nominal strain reaches at about 1.52%. After this point, the cementite layer starts to deform in elasto-plastic manner; however, the deformation is approximately uniform by the presence of ferrite layers as shown in Fig. 6(e) and stable deformation continues. Deformation process in three-layered specimen with ferrite5 is similar to the one with ferrite10, even though the period of stable plastic deformation in the cementite layer does not last long.

In contrast to the case with ferrite10 or ferrite5, three-layered specimens with ferrite5n or ferrite5n500 show sharp drops of nominal stress after their peak. This is due to the concentration of plastic deformation in the cementite layer when the strain-hardening ratio is low in the ferrite layers, which we observed in Fig. 6(b) or (c).

Results shown in Figs. 6 and 7 indicate as a whole that the strain hardening of ferrite layers contribute significantly to a stable plastic deformation of cementite layers and this effect is, in turn, assumed to originate from the presence of cementite layers: mutual constraint of deformation between soft and hard phases is playing a key role in the microstructure. It should also be noted again that high strength layers of ferrite with low strain hardening ability is not effective.

3.3 Stabilization of deformation by multi-layering

Pearlite colony [24] is basically composed of a number of parallel layers of ferrite and cementite. Deformation behaviors in layered structures could differ depending on the number of layers. In this section, we construct pearlite models that consist of 3, 5, 7, or 9 layers and analyze their deformation. Also in these models, central layers are cementite. Thicknesses of the ferrite and cementite layers are the same, except that the central layer of cementite is slightly thinned as described in the section 2, and they are simply piled up alternately. Specimens are subjected to tensile deformation in the horizontal direction by applying uniform tensile displacement on the both sides of the specimens. Mechanical properties of ferrite and cementite layers are those of ferrite-org and cementite shown in Table 1.

Fig. 8 shows development of the equivalent strain in layered structures with 3, 5, 7, or 9 layers, while in Fig. 9, distribution of equivalent plastic strain in the 7 layered specimen is shown when the nominal tensile strain is 1.527 %. In the three-layered model, shear

bands already develop when the nominal tensile strain is 1.5193% and this result is consistent with that shown in Fig. 3. In the five-layered model, shear bands develop when the nominal tensile strain increase from 1.525 to 1.527%; however we notice that plastically deformed region extends to wider area compared to the one in the three-layered model and the distribution of plastic strain in the ferrite layers is spreading widely, too. In the 7 or 9-layered models, the initial plastic deformation in the cementite layer does not show the appearance of the shear band and after such initial stage, plastic deformation gradually localizes. It is also noted that non-uniform deformation takes place not only in the first-nearest layers of the central cementite layer but also in the second- and third-nearest layers and beyond. Equivalent plastic strains in the cementite and ferrite layers differ largely (Fig. 9), while the equivalent strains in both layers are approximately the same (Fig. 8). This difference in plastic deformation in cementite and ferrite layers is compensated by elastic strain and this accompanies the difference in the stress state in both layers. From the results shown in Figs. 8 and 9, we understand that the deformation of the central cementite layer shifts to be a stable one by the presence of adjacent layers of ferrite and cementite.

Distribution of stress in the layered microstructure has been discussed from experimental [1] and theoretical [25] approaches. Fig. 10 shows distribution of equivalent stress in the 9-layered specimen. The maximum and the minimum values of the equivalent stress in the cementite layers are 2.75 GPa and about 2.7 GPa, respectively, while the stress in the ferrite layers is about 155 MPa, meaning that the stress partitioning in the cementite and ferrite is significant. During the initial stage of plastic deformation in the cementite layers, stress concentrates at around the plastically deformed area. After some plastic deformation in the cementite layer(s), area with the maximum value of the equivalent stress (=2.75 GPa) expands and the outmost layers of cementite bear the load more than the central layer.

Stabilization of plastic deformation by multiple layering shown in Figs. 8 and 9 looks to be a minor one compared to the effect by the change of mechanical response of ferrite layers, which we studied in the previous section. However, if the effects of multi-layering of ferrite and cementite and the change of mechanical properties of ferrite layers by the scale effect, or in other words the boundary effect [17,18], is combined, results could be even more significant. That is, it is considered that the localization of deformation is suppressed not only by a possibly higher yield stress and strain hardening in the ferrite layers, but also by multiple layering of ferrite and cementite.

In a fine lamellar microstructure of heavily drawn pearlite wire, a high concentration of carbon was observed in ferrite layers [26]. This increase in carbon concentration is assumed to change the yield stress and strain hardening behavior [18]. Generation of dislocations in the microstructure and their pileup and/or passage at ferrite/pearlite interfaces will also contribute largely to the mechanical response of the two phases [27]. Therefore, combined effect of geometrical, mechanical and chemical factors is

considered to contribute to the strong and, at the same time, ductile behavior of fine lamellar microstructure of pearlite.

In this study, we assumed that the plastic deformation of cementite was governed by the von Mises condition and associated flow rule. The plastic flow stress was set to be a constant, whereas the process of plastic deformation due to crystallographic slip [5,8] is another point of interest to be studied.

4. Summary

Fine lamellar structures of pearlite that consist of ferrite and cementite layers were modeled numerically and their elasto-plastic deformation were analyzed by two-dimensional finite element scheme. Results are summarized as follows.

1. Plastic deformation of bare cementite specimen was highly unstable under uniaxial tensile load.
2. Plastic deformation of cementite layer(s) was more or less stabilized by the presence of adjacent layers of ferrite and cementite, whereas a significant effect was observed when the yield stress and strain hardening rate of ferrite increased.
3. There was a tendency that unstable plastic deformation was suppressed when the number of layers of ferrite and cementite increased. This effect was assumed to originate from the fact that once a plastic deformation started in a small region of cementite, this induced alterations of stress state not only in the adjacent layers of ferrite but also in cementite and ferrite layers in far field, meaning that more than one cementite and ferrite layers bore larger external load.

Combined effect of the alteration of the mechanical properties of ferrite layers due to a scale effect and multiple layering could be a next point of discussion. Also a quantitative discussion on the alteration of mechanical response of ferrite layers is needed. Comparison of data from different approaches on the microscopic mechanical response of ferrite and cementite layers is left for further contribution.

Acknowledgement

This research was supported by Japan Science and Technology Agency (JST) under Collaborative Research Based on Industrial Demand "Heterogeneous Structure Control: Towards Innovative Development of Metallic Structural Materials".

References

[1] Y. Tomota, P. Lukáš, D. Neov, S. Harjo, Y.R. Abe, Acta Mat. 51 (2003) 805–817.

[2] M. Umemoto, Tetsu-to-Hagané 81 (1995) 157–166.

[3] M. Umemoto, K. Tsuchiya, Tetsu-to-Hagané 88 (2002) 117–128.

[4] T. Gladman, B. Hommes, F.B. Pickering, J. Iron Steel Inst. 208 (1970) 172.

[5] A. Inoue, T. Ogura, T. Masumoto, Trans. JIM 17 (1976) 663–672.

[6] M. Ojima, J. Inoue, S. Nambu, P. Xu, K. Akita, H. Suzuki, T. Koseki, Scripta Materialia 66 (2012) 139–142.

[7] M. Tanaka, Y. Yoshimi, K. Higashida, T. Shimokawa, T. Ohashi, Materials Science and Engineering, A submitted (2013).

[8] J. Gil Sevillano, Materials Science and Engineering 21 (1975) 221–225.

[9] J. Inoue, S. Nambu, Y. Ishimoto, T. Koseki, Scripta Materialia 59 (2008) 1055–1058.

[10] M. Serror, J. Inoue, J. Eng. Mech. 139 (2013) 94–103.

[11] www.ansys.com, ANSYS Mechanical, Release 13.0 (2010).

[12] J.R. Rice, Theoretical and Applied Mechanics, North-Holland, 1976.

[13] Z. Marciniak, K. Kuczynski, Int. J. Mech. Sci. 9 (1967) 609–620.

[14] Y. Adachi, S. Morooka, K. Nakajima, Y. Sugimoto, Acta Materialia 56 (2008) 5995–6002.

[15] Y.-T. Wang, Y. Adachi, K. Nakajima, Y. Sugimoto, Acta Materialia 58 (2010) 4849–4858.

[16] H.W. Swift, J. Mech. Phys. Solids 1 (1952) 1–18.

[17] J. Embury, R. Fisher, Acta Metallurgica 14 (1966) 147–159.

[18] X. Zhang, A. Godfrey, X. Huang, N. Hansen, Q. Liu, Acta Materialia 59 (2011) 3422–3430.

[19] N. Tsuji, Y. Ito, Y. Saito, Y. Minamino, Scripta Materialia 47 (2002) 893–899.

[20] M.D. Uchic, D.M. Dimiduk, J.N. Florando, W.D. Nix, Science 305 (2004) 986–989.

[21] A.R. Marder, B.L. Bramfitt, Met Trans A 7 (1976) 365–372.

[22] T. Ohashi, M. Kawamukai, H. Zbib, International Journal of Plasticity 23 (2007) 897–914.

[23] T. Ohashi, H.M. Zbib, Materials Science Forum 561-565 (2007) 1827–1832.

[24] T. Takahashi, M. Nagumo, Y. Asano, J. Japan Inst. Met. 42 (1978) 708–715.

[25] S. Sadamatsu, K. Higashida, Tetsu-to-Hagané 98 (2012) 328.

[26] T. Tarui, N. Maruyama, J. Takahashi, Nippon Steel Technical Report (2005) 56–61.

[27] T. Shimokawa, T. Oguro, M. Tanaka, K. Higashida, T. Ohshi, Materials Science and Engineering, A submitted (2013).

Table 1 Mechanical property of ferrite and cementite. Parameters *a*, *b* and *n* are used for Swift's equation and the parameter *c* is introduced in the modified Swift eq. (3). Data for ferrite-org and cementite are taken from Umemoto [2] and Umemoto and Tsuchiya [3], while data for ferrite5, ferrite10, ferrite5n and ferrite5n500 are hypothetical ones.

	Young's modulus [GPa]	Poisson's ratio	Yield stress [MPa]	*a* [MPa]	*b*	*n*	*c* [MPa]
cementite	181	0.3	2750				
ferrite-org	200	0.3	86.5	493	0.002	0.28	0
ferrite5	200	0.3	432.6	2465	0.002	0.28	0
ferrite10	200	0.3	865.2	4930	0.002	0.28	0
ferrite5n	200	0.3	348.1	493	0.002	0.056	0
ferrite5n500	200	0.3	848.1	493	0.002	0.056	500

Figure captions.

Fig. 1 Schematic illustration of a 5-layered pearlite model. Thickness at the mid part of the central layer of cementite is slightly thinned.

Fig. 2 Stress vs. strain relationship employed in this study for the cementite and five types of ferrite phase.

Fig. 3 Distributions of the plastic strain component $\varepsilon_{xx}^{(p)}$ in the bare cementite specimen when the nominal tensile strains are 1.500% (a), 1.504% (b) and 1.508% (c).

Fig. 4 Development of the plastic strain component $\varepsilon_{xx}^{(p)}$ at the central part of the layered specimen of ferrite-org/cementite/ferrite-org when the nominal tensile strains are (a) 1.5068%, (b) 1.5084%, (c) 1.5100% and (d) 1.5116%.

Fig. 5 Distribution of the normal plastic strain component $\varepsilon_{xx}^{(p)}$ in bare cementite

specimen (a) and ferrite-org/cementite/ferrite-org layered specimen (b). The nominal tensile strain is 1.7%.

Fig. 6 Distributions of the plastic strain component $\varepsilon_{xx}^{(p)}$ in five different specimen where the cementite layer is layered with (a) ferrite-org, (b) ferrite5n, (c) ferrite5n500, (d) ferrite5 and (e) ferrite10. The nominal tensile strain is 1.55%. Note that different color scales are used for (a), (b), (c) and (d), (e).

Fig. 7 Load-elongation curves of bare cementite and three-layered specimens.

Fig. 8 Distributions of the equivalent strain in 3, 5, 7 and 9 layered specimens. The central layer is cementite and is slightly thinned as described in the section 2. Layers of ferrite-org and cementite are stacked alternately. Number of layers and the nominal tensile strain are denoted as N and $\bar{\varepsilon}$, respectively.

Fig. 9 Distribution of plastic equivalent strain in the 7-layered specimen of ferrite-org and cementite when the nominal tensile strain is 1.527%. (a) and (b) are drawn from the same numerical result but displayed with different color scales to depict the distribution of plastic deformation in cementite and ferrite phases. Plastic deformations in cementite and ferrite layers differ largely and a larger elastic deformation in cementite and a smaller one in ferrite layers compensate this difference.

Fig. 10 Development of equivalent stress field in the 9-layered specimen. (a) and (b) are drawn from the same analysis results but displayed with different color scales to depict the stress field in each layers. Range of the equivalent stress in the cementite layers is approximately 2.7 to 2.75 GPa as shown in (a), while the value in ferrite layers is smaller than 157 MPa as shown in (b).

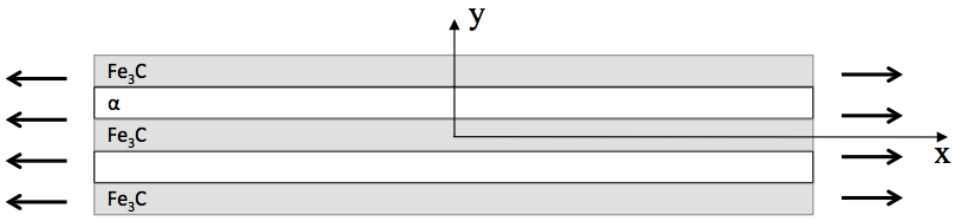

Fig. 1 Schematic illustration of a 5-layered pearlite model. Thickness at the mid part of the central layer of cementite is slightly thinned.

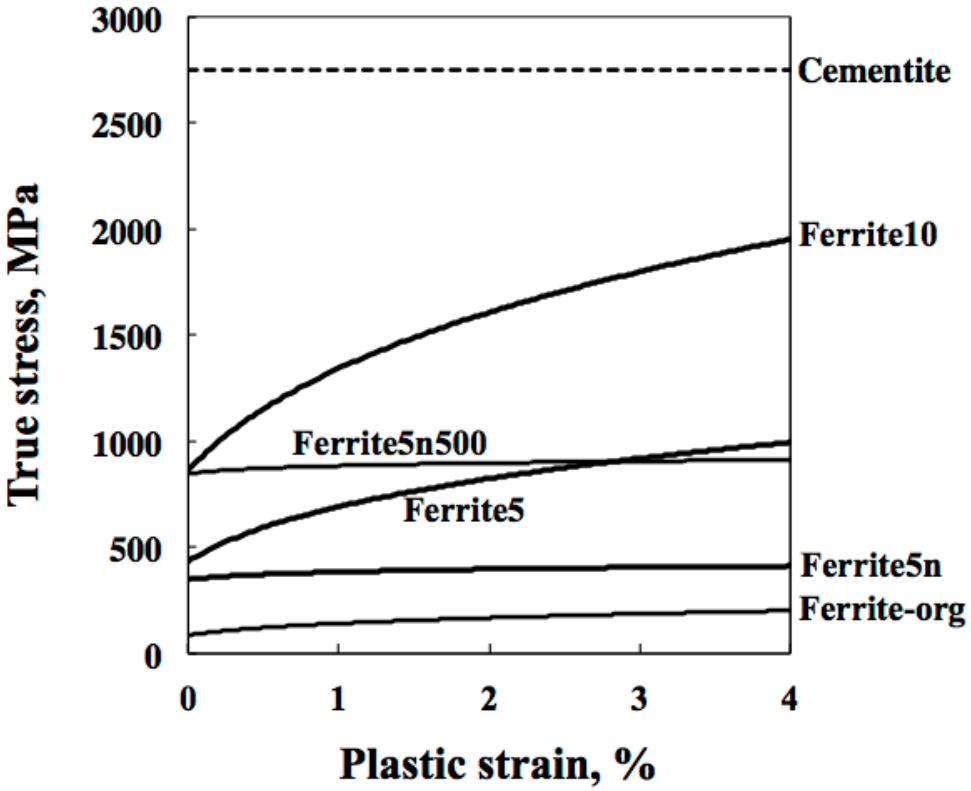

Fig. 2 Stress vs. strain relationship employed in this study for the cementite and five types of ferrite phase.

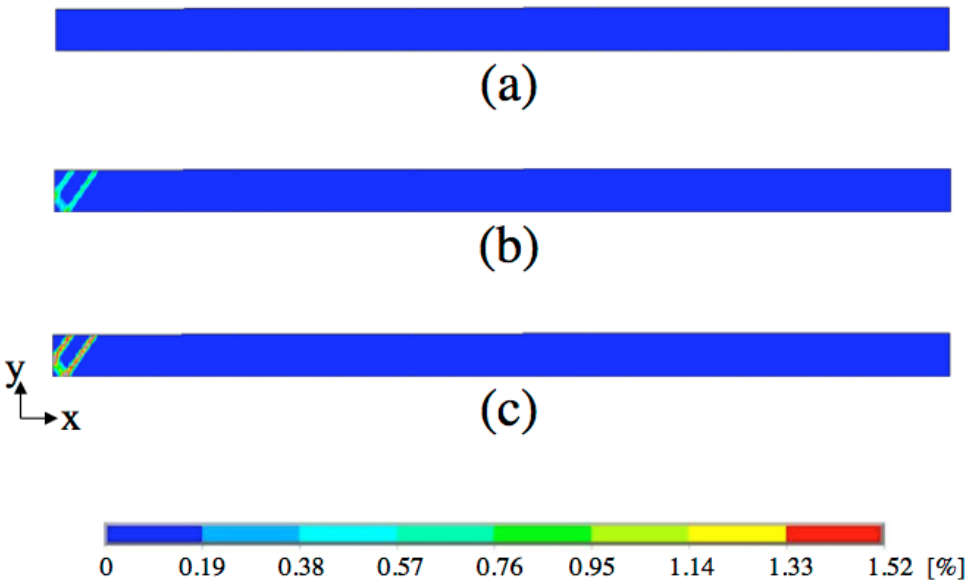

Fig. 3 Distributions of the plastic strain component $\varepsilon_{xx}^{(p)}$ in the bare cementite specimen when the nominal tensile strains are 1.500% (a), 1.504% (b) and 1.508% (c).

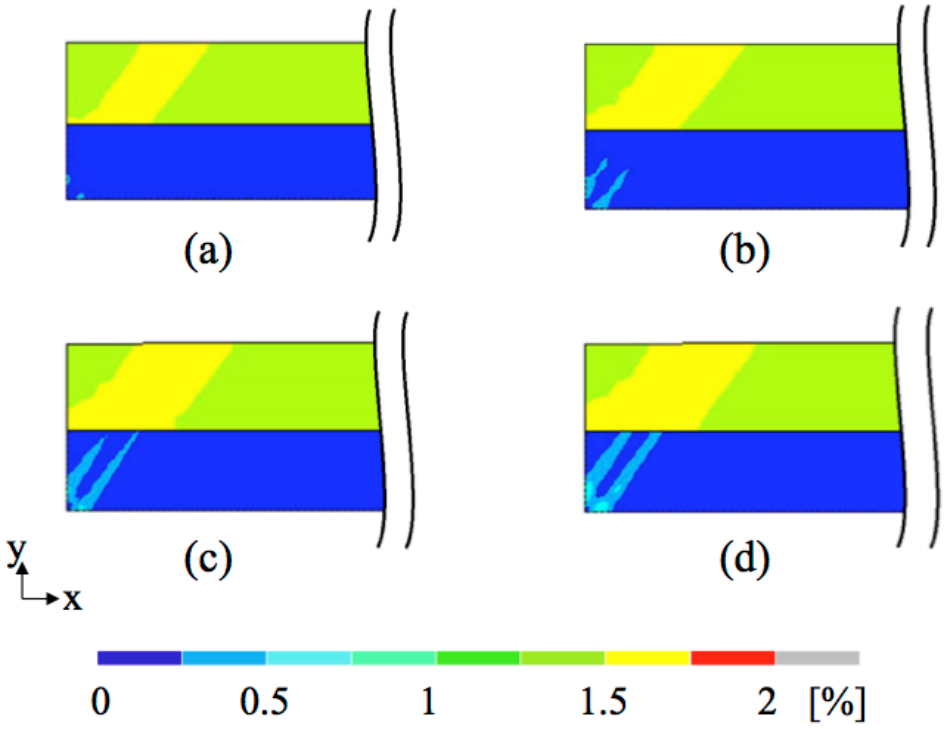

Fig. 4 Development of the plastic strain component $\varepsilon_{xx}^{(p)}$ at the central part of the layered specimen of ferrite-org/cementite/ferrite-org when the nominal tensile strains are (a) 1.5068%, (b) 1.5084%, (c) 1.5100% and (d) 1.5116%.

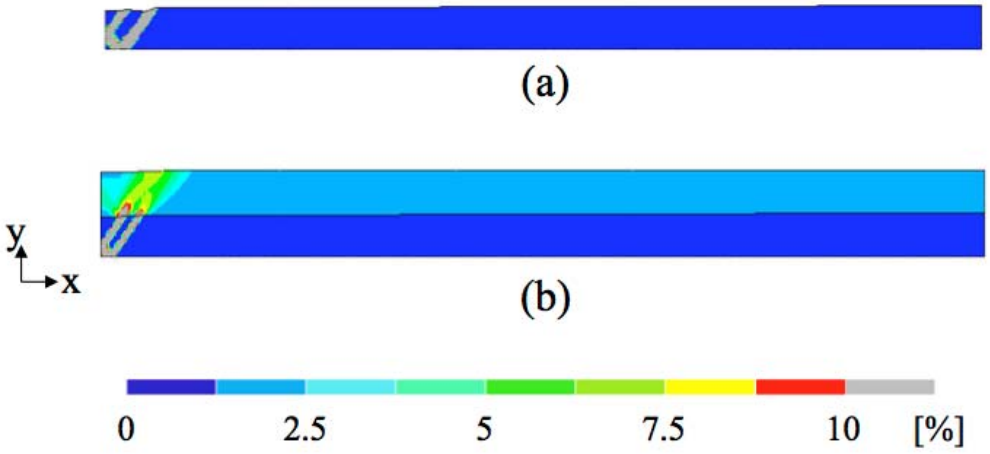

Fig. 5 Distribution of the normal plastic strain component $\varepsilon_{xx}^{(p)}$ in bare cementite specimen (a) and ferrite-org/cementite/ferrite-org layered specimen (b). The nominal tensile strain is 1.7%.

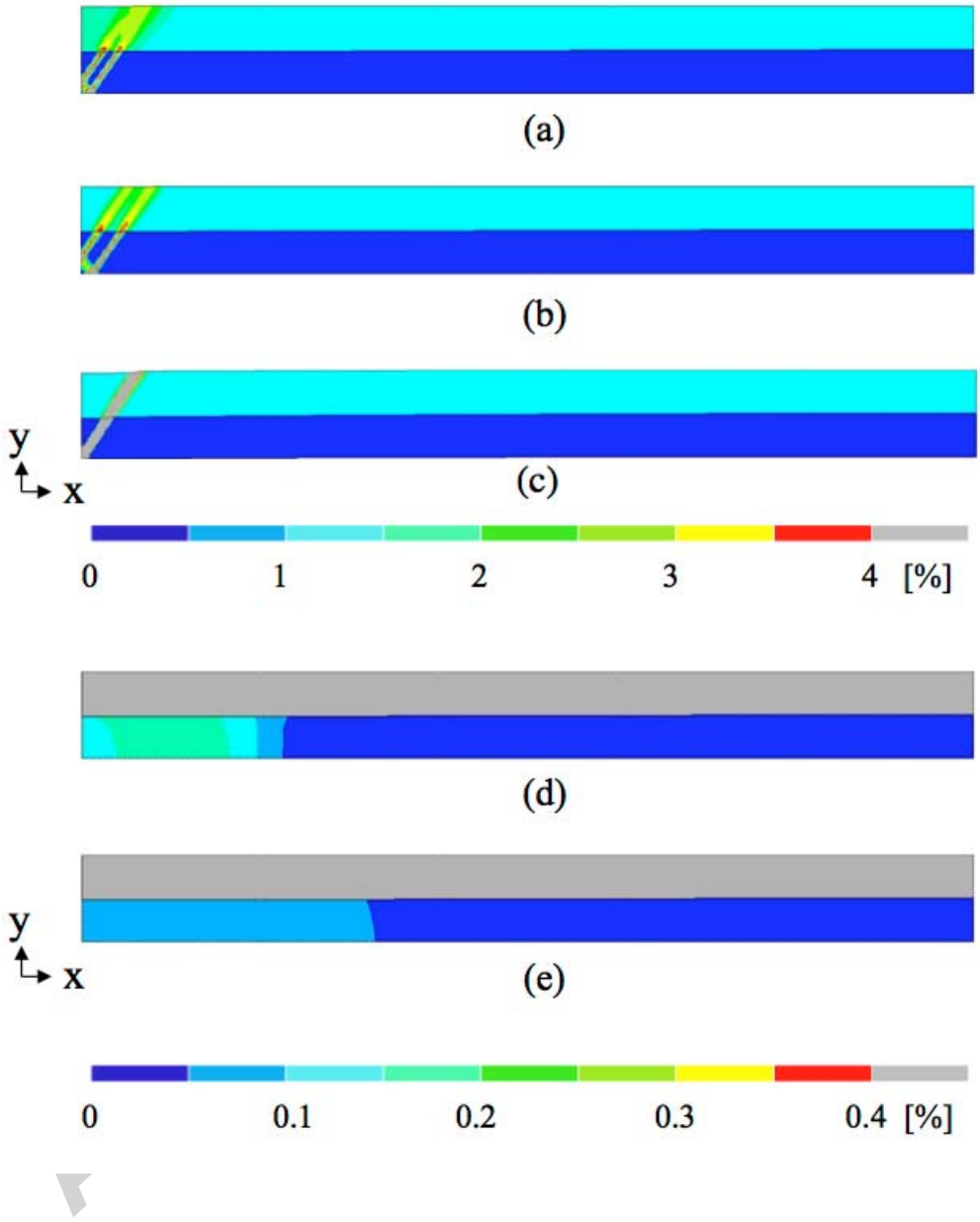

Fig. 6 Distributions of the plastic strain component $\varepsilon_{xx}^{(p)}$ in five different specimen where the cementite layer is layered with (a) ferrite-org, (b) ferrite5n, (c) ferrite5n500, (d) ferrite5 and (e) ferrite10. The nominal tensile strain is 1.55%. Note that different color scales are used for (a), (b), (c) and (d), (e).

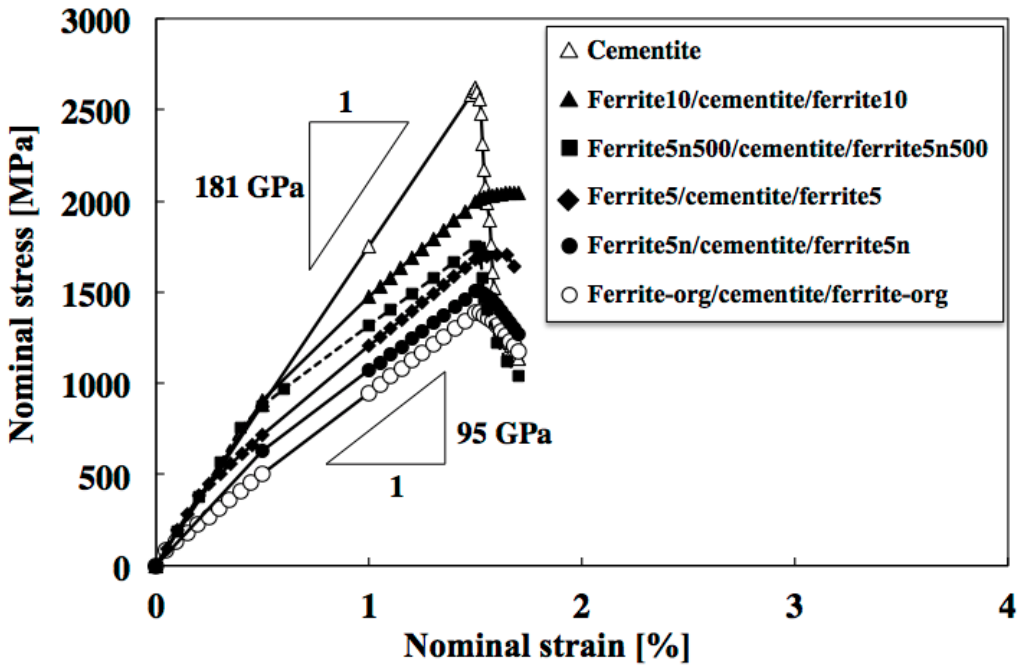

Fig. 7 Load-elongation curves of bare cementite and three-layered specimens.

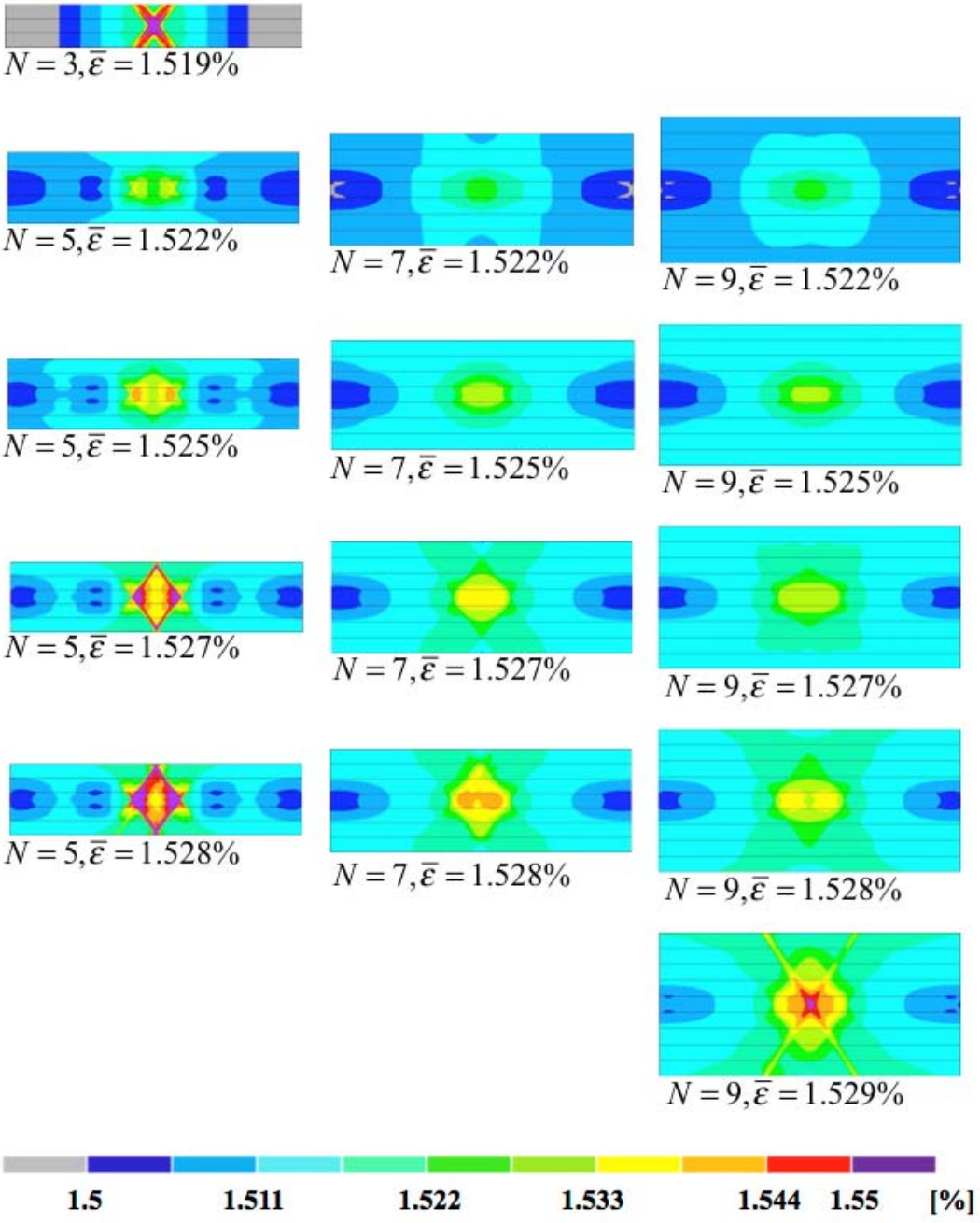

Fig. 8 Distributions of the equivalent strain in 3, 5, 7 and 9 layered specimens. The central layer is cementite and is slightly thinned as described in the section 2. Layers of ferrite-org and cementite are stacked alternately. Number of layers and the nominal tensile strain are denoted as N and $\bar{\varepsilon}$, respectively.

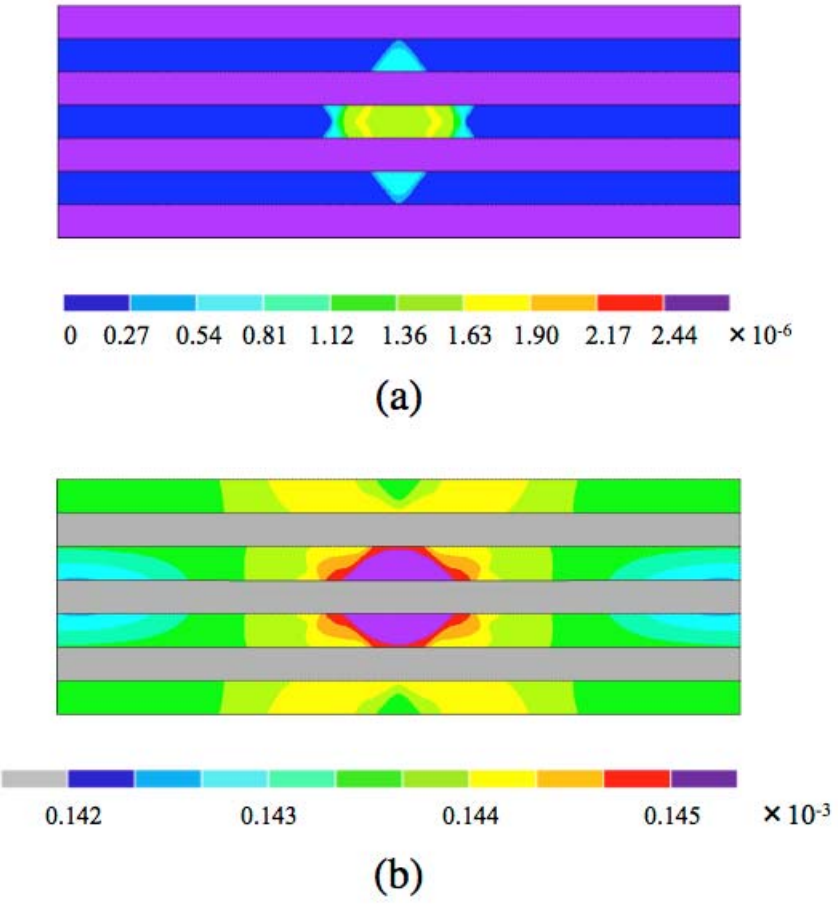

Fig. 9 Distribution of plastic equivalent strain in the 7-layered specimen of ferrite-org and cementite when the nominal tensile strain is 1.527%. (a) and (b) are drawn from the same numerical result but displayed with different color scales to depict the distribution of plastic deformation in cementite and ferrite phases. Plastic deformations in cementite and ferrite layers differ largely and a larger elastic deformation in cementite and a smaller one in ferrite layers compensate this difference.

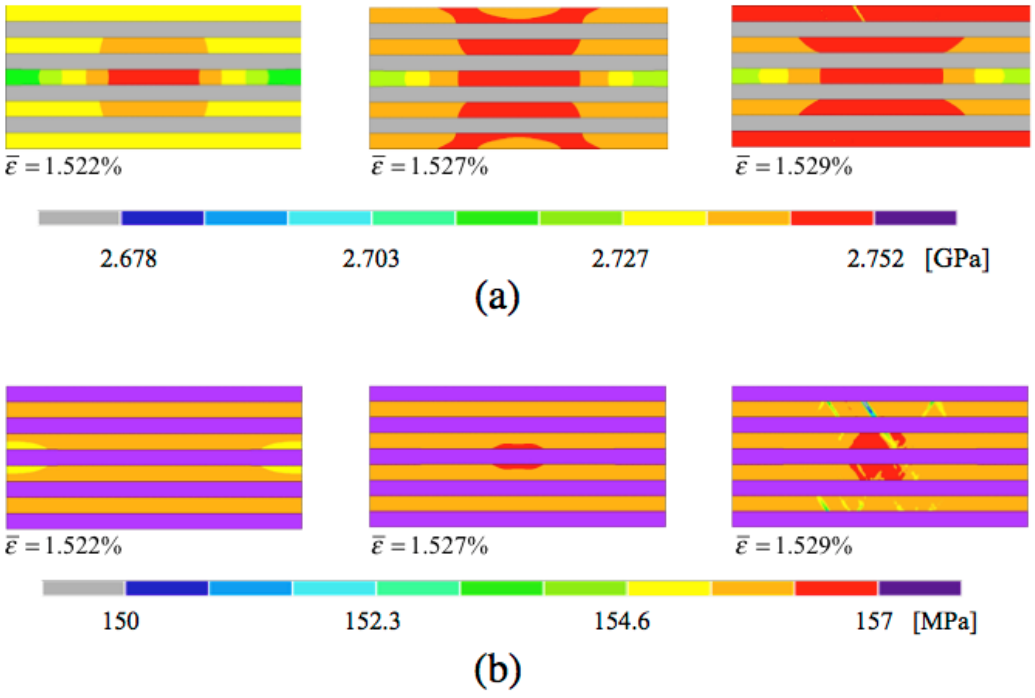

Fig. 10 Development of equivalent stress field in the 9-layered specimen. (a) and (b) are drawn from the same analysis results but displayed with different color scales to depict the stress field in each layers. Range of the equivalent stress in the cementite layers is approximately 2.7 to 2.75 GPa as shown in (a), while the value in ferrite layers is smaller than 157 MPa as shown in (b).